[講演概要(日本語)]

巨大地震の多様性とそれに応じた減災対策

カリフォルニア工科大学名誉教授
金森　博雄

地震学は広帯域地震学やGPSの発展によりこの３０年ほどの間に地震の発生様式を理解する上で長足の進歩をした。その結果、地震の震源スペクトラムの多様性が明らかになり、それに応じた防災対策が必要と考えられるようになった。ある地域の地震については将来の地震活動を地震やGPSのデータを用いて科学的に予測できるようになった。このような予測は長期の防災対策にはきわめて重要である。しかし破壊現象には偶発的な要素が多いので、そのような予測には大きな不確定性が伴い、たまには予期しないような地震が起こりうる。最近のリアルタイム地震学の発展によりそのような想定外の地震や津波にもある程度対処できるようになった。地震の多様性のよりよい理解と最新のリアルタイム技術を用いることが包括的な防災対策として最も重要である。

Review in Advance first posted online on January 15, 2014. (Changes may still occur before final publication online and in print.)

The Diversity of Large Earthquakes and Its Implications for Hazard Mitigation

Hiroo Kanamori

Seismological Laboratory, California Institute of Technology, Pasadena, California 91125; email: hiroo@gps.caltech.edu

Annu. Rev. Earth Planet. Sci. 2014. 42:7–26

The *Annual Review of Earth and Planetary Sciences* is online at earth.annualreviews.org

This article's doi: 10.1146/annurev-earth-060313-055034

Keywords

megathrust, tsunami earthquake, intraplate earthquake, moment-rate spectrum, high-rise building, tsunami warning

Abstract

With the advent of broadband seismology and GPS, significant diversity in the source radiation spectra of large earthquakes has been clearly demonstrated. This diversity requires different approaches to mitigate hazards. In certain tectonic environments, seismologists can forecast the future occurrence of large earthquakes within a solid scientific framework using the results from seismology and GPS. Such forecasts are critically important for long-term hazard mitigation practices, but because stochastic fracture processes are complex, the forecasts are inevitably subject to large uncertainty, and unexpected events will continue to surprise seismologists. Recent developments in real-time seismology will help seismologists to cope with and prepare for tsunamis and earthquakes. Combining a better understanding of earthquake diversity with modern technology is the key to effective and comprehensive hazard mitigation practices.

INTRODUCTION

Among the many advances in seismology in the past few decades are broadband seismology, GPS, and the rapid processing of data, which enable seismologists to determine the details of the rupture patterns of large earthquakes. Understanding such details is important for forecasting the general rupture behavior of large earthquakes in various subduction-zone environments. However, because of the stochastic nature of the rupture process, accurate short-term earthquake prediction is inevitably difficult. Fortunately, advancements in rapid data processing aided by modern computers enable seismologists to give real-time warning of tsunamis and earthquakes, which could save lives and properties, despite difficulties in short-term predictions. As our understanding of earthquake processes advances, we are learning of earthquake diversity, which requires different approaches to mitigate hazards. In this article I review the recent progress in understanding the diversity of large subduction-zone earthquakes and discuss future directions in research as well as the use of real-time seismology for hazard mitigation.

DIVERSITY OF EARTHQUAKES

Here I define diversity by the difference in the source radiation spectra of various earthquakes. It has long been known that some earthquakes are deficient and others are enriched in high-frequency radiation relative to commonly observed earthquakes. For example, the 1896 Sanriku, Japan, earthquake was not felt strongly, yet it generated one of the largest tsunamis in history. This earthquake was a slow rupture and was given the name tsunami earthquake (Kanamori 1972). The 1933 Sanriku earthquake, in contrast, is the largest ($M_w = 8.4$) recorded outer rise normal-fault earthquake, and the large ratio of the short-period body wave magnitude, m_B, to the longer-period surface wave magnitude, M_s, indicated strong high-frequency radiation (Kanamori 1971). These results were inevitably qualitative because of the limited instrumentation available, but the advent of broadband seismographs has allowed seismologists to quantitatively demonstrate great diversity in subduction-zone earthquakes. Lay et al. (2012) summarized these results, which are schematically shown in **Figure 1**, and introduced domains A, B, C, and D (though D is not shown in the figure). Ye et al. (2013) added domains I and II. Most large subduction-zone thrust earthquakes occur primarily in domain B over a depth range of 15 to 35 km. Domain A is a shallow part of the subduction zone where slow tsunami earthquakes occur. Domain C includes

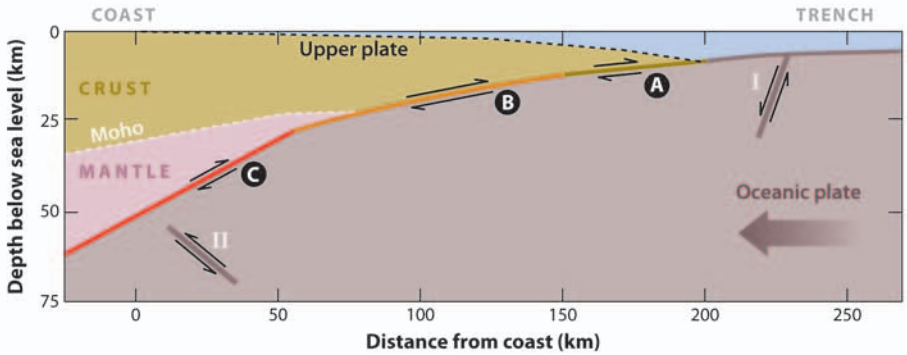

Figure 1

Rupture domains of subduction-zone earthquakes. Domains: A, near-trench domain; B, megathrust domain; C, downdip domain, where moderate earthquakes occur; I, outer rise (outer trench slope) domain; II, intraslab domain. Modified with permission from Lay et al. (2012) and Ye et al. (2013).

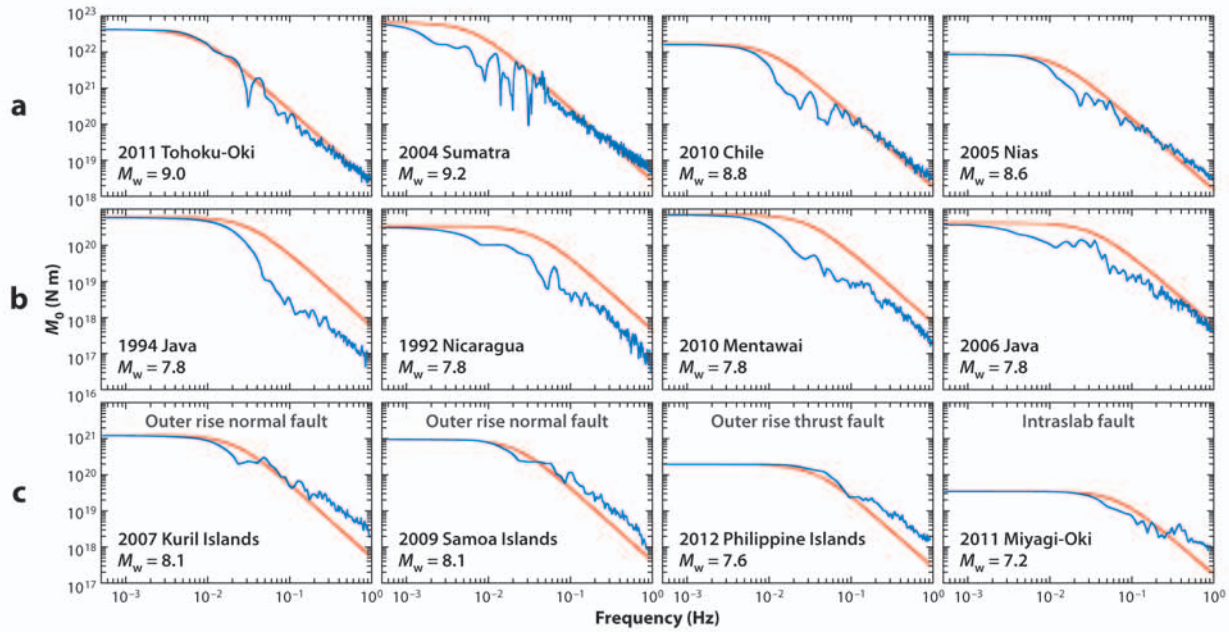

Figure 2

(*a*) Source spectra (*blue curves*) of domain B (megathrust) earthquakes. Each red curve indicates the reference spectrum for the event with the given magnitude. (*b*) Source spectra of domain A (tsunami) earthquakes. Note the lower spectral amplitude at high frequencies (short periods). (*c*) Source spectra of intraplate earthquakes. Note the enhanced spectral amplitude at high frequencies (short periods).

relatively small slip patches where moderate-sized thrust earthquakes occur. Domain D represents the location where very slow slips and tremors occur in some subduction zones. Domains I and II are intraplate domains in the outer rise (outer trench slope) region and within the subducted slab, respectively. Here we focus on domains A, B, I, and II, where large, often very damaging earthquakes occur. Lay et al. (2012) and Ye et al. (2013) discuss all these domains in detail. Large earthquakes occasionally occur in the upper plate, but they are seldom as large as those in the domains shown in **Figure 1** and are not discussed in this paper.

Figure 2 illustrates the diversity in terms of the source spectrum (more precisely, the moment-rate spectrum), $|\hat{\dot{M}}_0(f)|$, of several recent large earthquakes as a function of frequency f. **Figure 2** shows the source spectrum of earthquakes in domain B, domain A, and domains I and II. The moment-rate spectrum is obtained from broadband P waveforms at many stations. The red curves in **Figure 2** represent a reference spectrum given by

$$|\hat{\dot{M}}_0(f)| = \frac{M_0 f_c^2}{(f^2 + f_c^2)}, \tag{1}$$

where M_0 is the seismic moment and f_c is the corner frequency, given by $f_c = 0.49\beta(\frac{\Delta\sigma_r}{M_0})^{1/3}$. Here, $\Delta\sigma_r$ is a scaling parameter with the dimension of stress. We set $\beta = 3.75$ km/sec and $\Delta\sigma_r = 3$ MPa. This spectral shape, called the ω^2 spectrum, was suggested by Brune (1970) and Aki (1967). The numerical values of β and $\Delta\sigma_r$ do not carry a distinct physical meaning, but they are used to scale the spectra of earthquakes with different sizes. The basic scaling of the spectrum is given by $f_c \propto M_0^{-1/3}$, which has been shown to be one of the general scaling relations for earthquakes (e.g., Kanamori & Anderson 1975). As shown in **Figure 2**, the ω^2 spectrum can represent well

the overall spectral shape, but the spectral amplitude relative to that of the reference spectrum at high frequency is different for events in different domains, reflecting the diversity.

Domain B Earthquakes

Most large subduction-zone thrust earthquakes occur in domain B. Some of the most significant earthquakes, most notably the 2011 Tohoku-Oki earthquake ($M_w = 9.0$), nucleated in domain B, and the rupture extended into domains A and C. Yomogida et al. (2011) discussed the importance of interactions between different domains for understanding the rupture behavior of great earthquakes. Domain B earthquakes occur on the subduction-zone megathrust that is locked during the interseismic period. As the shear stress on the boundary increases and exceeds the local strength, a rupture occurs, and the stress drops. In this case, if we know the strain loading rate, $\dot{\varepsilon}$, and the average strain drop in earthquakes, $\Delta\varepsilon$, we can estimate the average repeat time of these earthquakes. The strain (loading) rate $\dot{\varepsilon}$ varies for different plate boundaries, but recent GPS studies indicate that the rate is on the order of $\dot{\varepsilon} \approx 1$ to 2×10^{-7}/year for the subduction zones in Japan (e.g., Sagiya 2004). A similar rate has been estimated for other major plate boundaries (e.g., Hackl et al. 2009). The estimation of the strain drop of earthquakes dates back to Tsuboi's (1932) study of the 1927 Tango earthquake. He estimated $\Delta\varepsilon$ to be approximately 10^{-4}. More recent studies indicate that $\Delta\varepsilon$ for large earthquakes falls within a range of 2×10^{-5} to 2×10^{-4}, with some outliers. If we use $\dot{\varepsilon} \approx 2 \times 10^{-7}$/year as a representative value, then the repeat time of large subduction-zone earthquakes is on the order of $\tau = \Delta\varepsilon/\dot{\varepsilon} \approx 100$ to 1,000 years. As I discuss below, this relatively short repeat time enables seismologists to make useful forecasts of domain B earthquakes.

Figure 3*a* shows a schematic view of the regional variations in the rupture zones of domain B earthquakes. Press (1961) demonstrated from rupture directivity that the 1960 great Chilean earthquake ($M_w = 9.5$) ruptured over a distance of as long as 1,000 km. This is consistent with the long aftershock area (Saint-Amand 1961). Also, the asymmetric radiation pattern of long-period waves clearly indicates that the 1964 Alaskan earthquake ($M_w = 9.2$) ruptured over a large distance of 600 km (Kanamori 1970). These observations suggest that these subduction

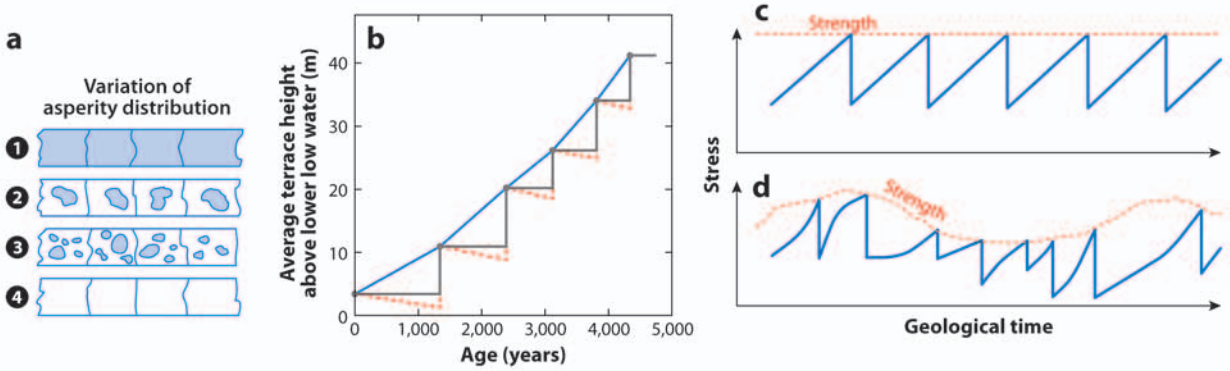

Figure 3

(*a*) Schematic diagram showing the regional variation of asperity (slip patch) distributions. Modified with permission from Lay & Kanamori (1981). (*b*) The heights measured from lower low water of six terraces at Middleton Island in Alaska as a function of age (Plafker & Rubin 1978). The solid gray curve shows an inferred uplift sequence assuming no interseismic vertical movement. The dashed red line assumes some interseismic subsidence. The solid blue line indicates the average uplift rate between terraces. (*c*) Schematic diagram showing an end-member earthquake sequence with regular occurrence. (*d*) Irregular earthquake sequence caused by asperity interactions.

zones have an extended slip on a strongly coupled zone, which is called an asperity. Studies on large earthquakes in other subduction zones have shown that the asperity size and distribution seem to vary for different subduction zones, as is schematically shown in **Figure 3*a*** (Lay & Kanamori 1981). When the rupture zone is characterized by a large asperity with a distinct length scale such as that in **Figure 3*a***, case 1, one would expect a relatively regular sequence of great earthquakes on essentially the same asperity. In fact, in southern Chile, large earthquakes have occurred in a relatively regular sequence (Lomnitz 2004), though considerable variability among these events has been reported (Cisternas et al. 2005). At Middleton Island in Alaska, six marine terraces with height ranging from 3.5 to 9 m indicate coseismic uplifts with a recurrence time of 500 to 1,350 years (**Figure 3*b***) (Plafker & Rubin 1978). If we simplify this type of sequence, the stress accumulation and release process can be expressed by a simple saw-tooth diagram, as shown in **Figure 3*c***. Seismologists at Tohoku University observed a unique sequence like this near Kamaishi, Japan, where 11 $M \approx 5$ earthquakes occurred regularly with an average repeat time of six years (e.g., Uchida et al. 2007). They hypothesized that these earthquakes ruptured a small, isolated asperity surrounded by a creeping zone where the plates are continuously slipping.

In contrast to case 1 in **Figure 3*a***, if the variously sized asperities are distributed randomly, as they are in case 3, different patches may have complicated interactions that result in a complex irregular seismic sequence, as shown in **Figure 3*d***. Here, interaction means interasperity triggering. When one asperity fails, the resulting stress perturbation may or may not trigger the adjacent asperities. This type of interaction was noted in doublet earthquakes in the Solomon Island region (Lay & Kanamori 1980).

The behavior of mechanical systems controlled by interactions of asperities without distinct length scale is characterized by a power law between the energy and event frequency, and this has been shown by many investigators (e.g., Otsuka 1972, Vere-Jones 1976, Bak & Tang 1989). This relation has long been known in seismology as the Gutenberg–Richter relation. In this case, it is difficult to make a deterministic forecast of events. Only the general behavior of seismicity can be statistically predicted.

Thus, two end members of the earthquake process can be considered. One is a deterministic process governed by asperities with well-defined sizes, and the other is a more chaotic process governed by the interaction of asperities without any distinct scale. The real earthquake sequence is intermediate between these two end members. If the plate boundary structure is simple, as it is in **Figure 3*a***, case 1, earthquakes can occur with a characteristic size and time, which allows forecasts with some confidence. If the plate boundary is complex, as it is in **Figure 3*a***, case 3, it is difficult to make a deterministic forecast. Thus, depending on the tectonic environments of earthquakes, we need to take different approaches to mitigate hazards. Although the asperity structures are more complex than those in **Figure 3*a***, we use that overall characterization to develop conceptual models for effective hazard mitigation.

Domain A Earthquakes

Domain A earthquakes occur in a narrow zone along the trench and are usually smaller than domain B earthquakes. These events are generally called tsunami earthquakes because they generate disproportionately large tsunamis for their seismic magnitude. Although shaking damage is usually minor, tsunami damage is often extensive (Kanamori 1972; Kanamori & Kikuchi 1993; Newman & Okal 1998; Polet & Kanamori 2000, 2009).

As shown in **Figure 2*b***, the source spectra of several recent tsunami earthquakes consistently show deficiency in high-frequency radiation for a given moment. Because domain A earthquakes are located far from the coast, it is difficult to locate the rupture zone accurately. It is difficult to

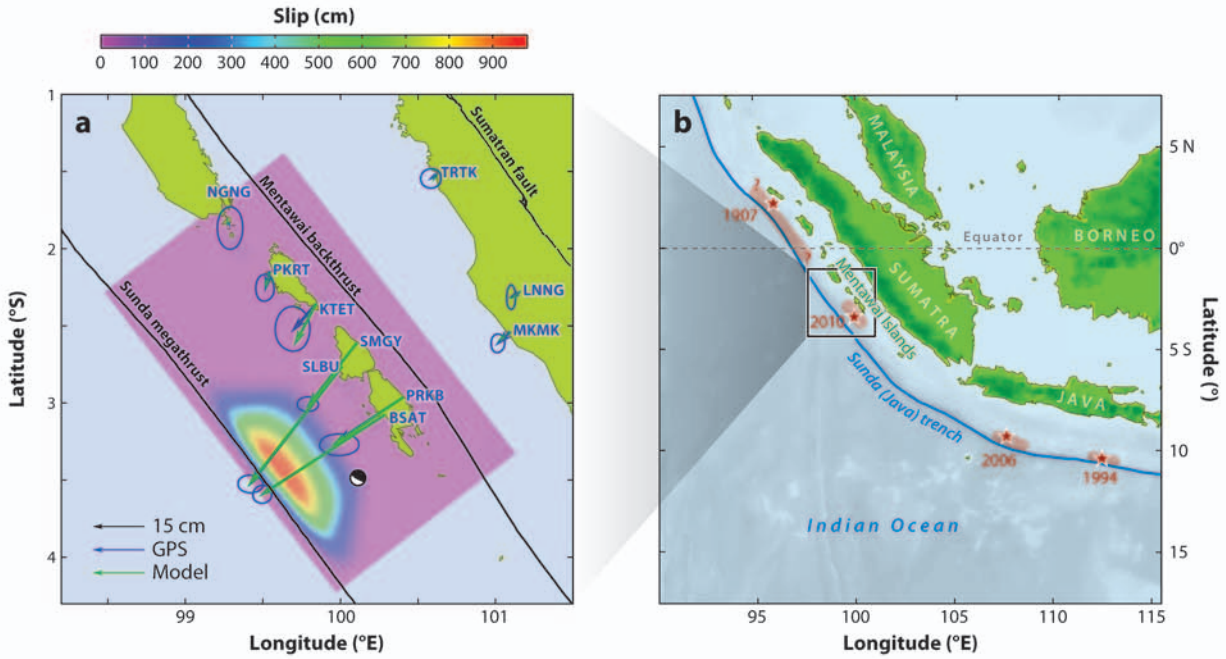

Figure 4

(*a*) The rupture zone of the 2010 Mentawai, Sumatra, tsunami earthquake (Hill et al. 2012). The focal mechanism of the 2010 Mentawai earthquake is denoted by the black and white half-moon symbol. The blue abbreviations denote the Sumatran GPS Array (SuGAr) station names. (*b*) Tsunami earthquakes along the Sunda arc (Lay et al. 2011).

determine how narrow the rupture zone is and how close it is to the trench. However, for the 2010 Mentawai, Sumatra, tsunami earthquake (Newman et al. 2011, Lay et al. 2011), Hill et al. (2012) took advantage of the GPS and tsunami observation at the islands in the forearc (between the coast and trench) and demonstrated that the rupture zone is indeed very narrow along the trench (**Figure 4*a***).

When the narrow zone along the trench ruptures by itself, the event exhibits clear characteristics of tsunami earthquakes, but in the case of great earthquakes, such as the 2011 Tohoku-Oki earthquake and possibly the 2004 Sumatra earthquake, a rupture in domain B triggered a slip in domains A and C so that the event as a whole did not obviously exhibit the characteristics of tsunami earthquakes. This is mainly because high-frequency radiation from domains B and C and low-frequency radiation from domain A cannot be separated.

As many domain A events have been studied recently, especially those along the Sunda arc off the coast of Sumatra and Java, an interesting feature has emerged, shown in **Figure 4*b***. This figure shows the rupture zones of four tsunami earthquakes along the Sunda arc—the 1907 Sumatra earthquake (Newcomb & McCann 1987, Kanamori et al. 2010), the 1994 Java earthquake (Abercrombie et al. 2001, Polet & Thio 2003), the 2006 Java earthquake (Ammon et al. 2006), and the 2010 Mentawai Island earthquake. The result for the 1907 event is only qualitative because of the limited data available at that time. Although there is no direct evidence that only the narrow zone along the trench ruptured, macroseismic reports on the extent of the tsunami, a relatively small seismic magnitude (M = 7.5 to 8), and the earthquake's spatial relation to the 2005 Nias earthquake (domain B event; Hsu et al. 2006) suggest that it was a domain A event similar to, but much larger than, the other domain A events along the Sunda arc. It is also somewhat similar to

the 2011 Tohoku-Oki earthquake. The 2005 Nias earthquake ($M_w = 8.5$) and the 2007 Sumatra earthquake ($M_w = 8.4$) (Konca et al. 2008) ruptured in domain B and did not seem to rupture in domain A. Thus, domain A and B earthquakes appear to have their own spatial and temporal sequences. Newcomb & McCann (1987) and Sieh et al. (e.g., Sieh et al. 2008) suggest that the domain B events along the Sunda arc have repeat times of 150 to 200 years. However, the average repeat time for domain A events is not known, partly because these events occur less frequently than domain B events do. It is not even clear whether domain A events occur with any regularity. Until recently, it was generally believed, without much hard evidence, that the plate coupling near the trench is only partial (i.e., a significant fraction of slip is in aseismic creep), and the repeat time there can be much longer and possibly irregular. Philibosian et al. (2012) suggested, on the basis of long-term uplift evidence from coral studies, that the shallow Sunda megathrust has its own sequence with much longer repeat times, on the order of 1,000 years. Prior to the 2011 Tohoku-Oki earthquake, in which the large slip of more than 50 m occurred in the shallow megathrust near the trench, no comparable great earthquake was known to have occurred in the same zone for at least 1,000 years. If this long repeat time is characteristic of domain A earthquakes, it would be very difficult to reliably forecast them.

Intraplate Events

Great normal-fault earthquakes occur within outer rise or outer trench slope regions. Although they are not as frequent as domain B megathrust earthquakes, they pose significant tsunami and shaking hazards. Outer rise normal-fault earthquakes were first noticed by Stauder (1968a,b) along the Aleutian arc and were deemed the result of extensional stress caused by plate bending upon subduction. These are relatively small events ($M \leq 7$). Subsequently, a much larger ($M_w = 8.4$) normal-fault earthquake was found off the Sanriku Coast of Japan. This event caused significant tsunami damage, with a death toll of about 3,000. Only four outer rise normal-fault earthquakes with $M_w \geq 8$ have been instrumentally recorded: the 1933 Sanriku earthquake ($M_w = 8.4$), the 1977 Sumbawa earthquake ($M_w = 8.3$; Spence 1986, Lynnes & Lay 1988), 2007 Kuril Islands earthquake ($M_w = 8.1$; Ammon et al. 2008), and the 2009 Samoa Islands earthquake ($M_w = 8.0$; Beavan et al. 2010, Lay et al. 2010b). Enhanced high-frequency radiation was qualitatively noticed for both the 1933 Sanriku and the 1977 Sumbawa earthquakes and was quantitatively confirmed for both the 2007 Kuril Islands earthquake and the 2009 Samoa Islands earthquake, as shown in **Figure 2*c***.

In the outer rise region, large earthquakes with thrust mechanisms also occur (Christensen & Ruff 1988). They occur at a depth of 40 km or deeper in the oceanic plate and can be interpreted mainly as a result of compressional stress due to bending. They are generally smaller, and even less frequent, than the normal-fault earthquakes; the largest recorded event is $M_w = 7.6$. A recent event in the Philippines (August 31, 2012, $M_w = 7.6$) offshore Leyte is a typical example (Ye et al. 2012). Its source spectrum is also enhanced in high frequency, as shown in **Figure 2*c***. Ye et al. (2013) called these groups of events domain I events (see **Figure 1**). Because of the enhanced excitation at high frequency, these events have important implications for strong-motion hazards and should be given special attention in ground-motion studies. A comparison of the 2007 Kuril Islands earthquake (domain I, outer rise normal-fault earthquake) with the 2006 Kuril Islands megathrust earthquake (domain B, $M_w = 8.3$), which occurred about two months prior to the 2007 outer rise earthquake, presents a good case (see **Figure 5*a***) (Ammon et al. 2008). **Figure 5*b*,*c*** compares the source spectrum and the strength of ground motions along the Japanese Islands. Although the 2007 event was smaller than the 2006 event in M_w determined at the long period, its ground motion at high frequency was about five times larger.

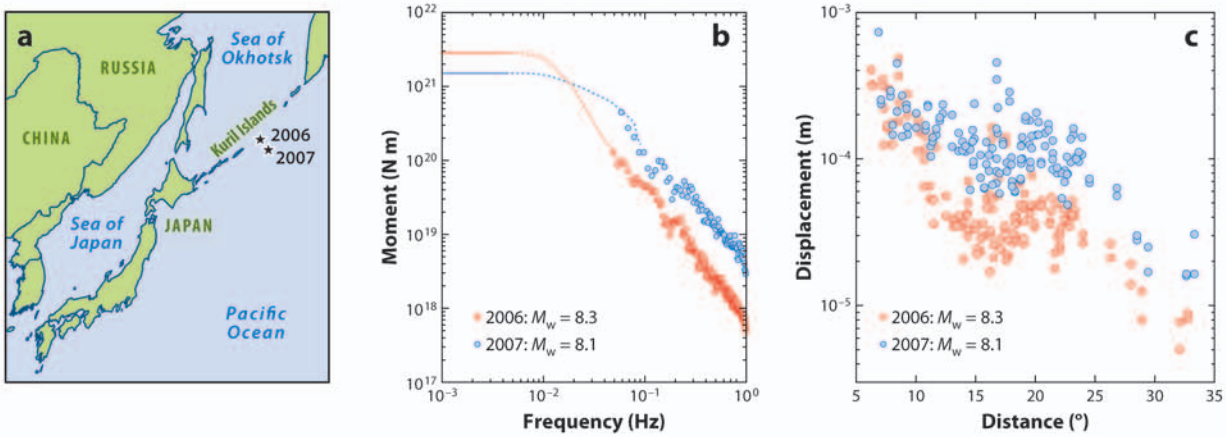

Figure 5

Comparison of ground motions of two Kuril Islands earthquakes in 2006 (M_w = 8.3, domain B) and 2007 (M_w = 8.1, domain I). (*a*) Locations of the two events. (*b*) Source spectra of the two events (Ammon et al. 2008). The blue and red solid lines indicate the seismic moment of the 2007 and 2006 Kuril Islands earthquakes, respectively. The blue and red dashed lines schematically connect the moment and the spectrum. (*c*) Ground-motion amplitudes along the Japanese island. Northeast- and southwest-component ground-motion displacements filtered over a pass-band from 0.167 to 0.3 Hz (6 to 3.3 sec) are shown. Abbreviation: JMA, Japan Meteorological Agency.

Another class of intraplate events in subduction zones, domain II earthquakes, includes events that occur at a depth of 50 to 150 km within the subducted oceanic plate. A recent example is an M_w = 7.1 earthquake that occurred on April 7, 2011, after the 2011 Tohoku-Oki earthquake (Nakajima et al. 2011, Ohta et al. 2011). Despite its relatively small M_w, it caused very strong shaking near Sendai. As shown in **Figure 6**, the peak ground-motion acceleration caused by this event was comparable to, or even larger than, that of the M_w = 9.0 mainshock at some locations. This underscores the impact of this type of earthquake on ground-motion studies. The source spectrum of this earthquake (**Figure 2*c***) is similar to those of the outer rise earthquakes, with enhanced excitation at high frequency. Ye et al. (2013) conducted a detailed study of ground-motion characteristics of this event at even higher frequencies. Although there has not been a thorough global systematic study of this type of earthquake, these intraplate events are generally known to cause very strong shaking in the epicentral area (e.g., Ide & Takeo 1996, Suzuki et al. 2009, Asano et al. 2004, Morikawa & Sasatani 2003), and they can have significant hazard potential. The 1939 Chillán, Chile, earthquake was probably of this type (M_s = 7.8, depth = 80 to 100 km; Beck et al. 1998) and was one of the most damaging earthquakes in Chile.

The mechanism of these intraslab earthquakes is not directly controlled by plate motion. It is controlled by whether the stress in the slab is down-dip tension or down-dip compression; as a result, the mechanism can be either thrust or normal-fault. For example, the April 7, 2011, Miyagi-Oki event was a thrust, but the 1939 Chillán earthquake was a normal-fault.

Because both outer rise earthquakes and the events within subducted plates are not directly controlled by relative plate motion, the repeat times for these events are not known. It is even unclear whether we can expect any systematic repeating behavior.

EARTHQUAKE FORECAST

Forecast of subduction-zone earthquakes has long been attempted by many investigators. One of the most notable examples is that of Imamura (1928), who studied the spatial distribution of large

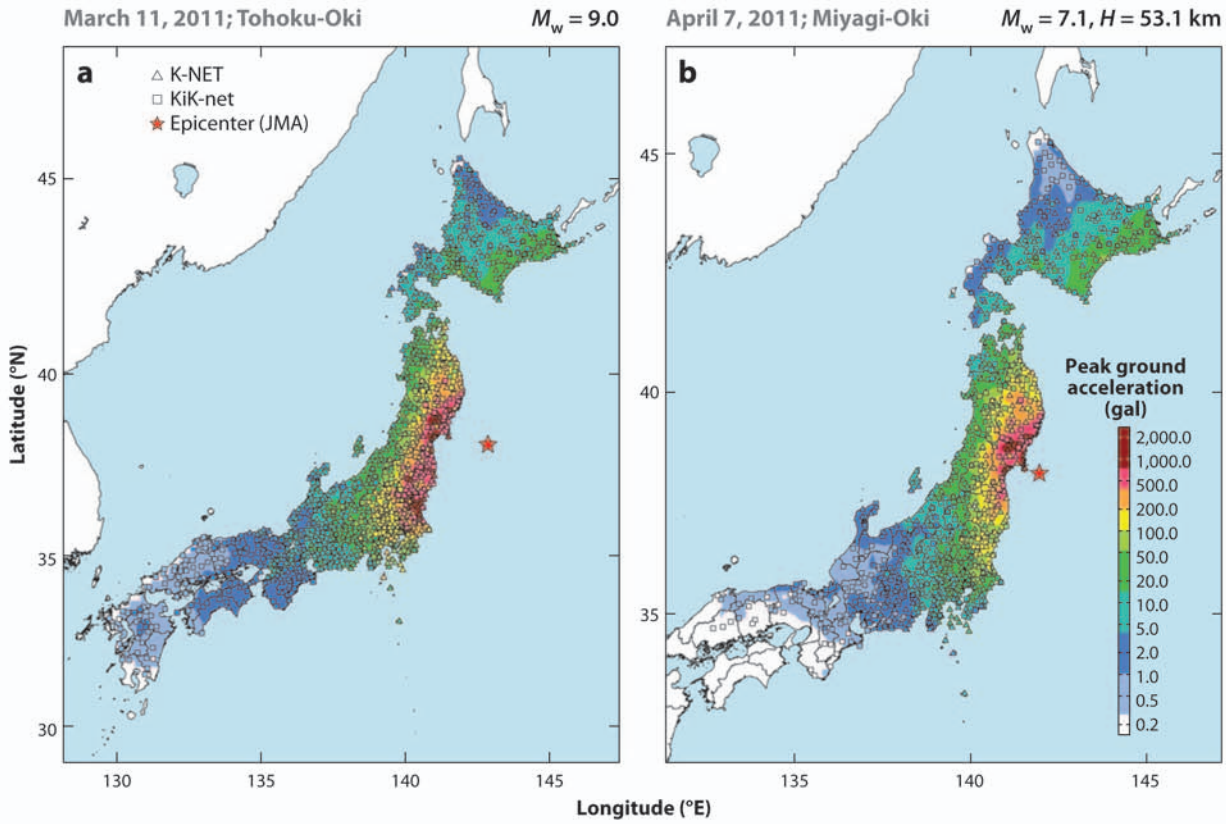

Figure 6

Peak ground-motion acceleration caused by (*a*) the 2011 Tohoku-Oki mainshock (M_w = 9.0) and (*b*) the 2011 Miyagi-Oki intraslab earthquake (M_w = 7.1) (**http://www.kyoshin.bosai.go.jp/kyoshin/quake/**).

damaging earthquakes in southwest Japan using historical documents. By analyzing the records of historical events, especially those in 1498, 1605, 1707, and 1854, he concluded that they tend to occur at intervals between 100 and 150 years. In 1928, when he wrote his paper, 74 years had elapsed since the last earthquake. Imamura anticipated the imminent occurrence of another major event and started seismic and geodetic monitoring of the area. Unfortunately, his effort was discontinued because of World War II, but the anticipated earthquake did occur in 1944 (Tonankai earthquake, M_w = 8.0), and another occurred in 1946 (Nankaido earthquake, M_w = 8.1). This type of forecast was further promoted by Fedotov (1965) and Mogi (1968) and, since the advent of plate tectonics, by Sykes (1972), Kelleher et al. (1974), Ando (1975), McCann et al. (1979), and others in the framework of the seismic gap. Although the validity of probabilistic assessment of seismic gaps has been debated (Kagan & Jackson 1991, Nishenko & Sykes 1993), a better understanding of the strain accumulation and release process forms the basis of scientific earthquake forecasting.

For scientific forecasts we need to know the following: (*a*) the field (in the sense of physics), (*b*) the boundary and initial conditions, (*c*) the field variables, and (*d*) the governing equations. Here, the field is a subduction zone, and the boundary and initial conditions are determined by the plate geometry and past seismic activity. The field variables include the plate convergence rate, the plate coupling factor, and the variables associated with asperities and frictional properties

(i.e., constitutive relations). The governing equations are mainly based on the theory of elasticity. Needless to say, all of these elements are subject to large uncertainties, but the advent of GPS and broadband seismology, along with a better understanding of the frictional characteristics of the plate boundary interface, has allowed seismologists to advance the earthquake forecasting pioneered by Imamura to a methodology in a more rigorous scientific framework.

A good example of forecasting is that used for the 2010 Maule, Chile, earthquake (domain B, $M_w = 8.8$). The earthquake occurred on the Chilean megathrust, where another large earthquake had occurred in 1835 ($M \approx 8$ to 8.5) (see **Figure 7*a***). Charles Darwin experienced this earthquake and wrote a first-hand account of it in his 1845 book (Darwin 1845). Since that time, no major earthquake had occurred on this segment, called the Charles Darwin gap. The 1939 event was not a megathrust event (Beck et al. 1998). The average repeat time of Chilean megathrust earthquakes is estimated to be 100 to 200 years. Thus, in the 1990s, the Charles Darwin gap was expected to host another large earthquake in the near future. These are the boundary and initial conditions to be used for forecasting the seismic activity in this gap. Having realized these conditions, several investigators began taking GPS measurements in this general area in 1996 (e.g., Ruegg et al. 2002). On the basis of the displacement field determined by the 10-year GPS survey, Ruegg et al. (2009) concluded that if the plate coupling has been 100% since 1835, there was approximately 10 m of slip deficit along this gap (slip deficit is the amount of slip that would occur if the accumulated strain were released in an earthquake); they forecasted that an $M_w = 8.5$ earthquake would occur if the gap ruptured soon. Then, on February 27, 2010, a $M_w = 8.8$ earthquake did occur in the expected area with the expected mechanism (see **Figure 7*a***) (e.g., Lay et al. 2010a, Delouis et al. 2010, Lorito et al. 2011, Vigny et al. 2011). The magnitude was slightly larger than forecasted, but this much uncertainty is inevitable considering all the complexities of the subduction-zone structures and the stochastic elements associated with fracture phenomena like earthquakes. By most standards, this should be considered a successful forecast on the basis of scientific data and methodology.

A very similar forecast was made for the 2012 Costa Rica earthquake (domain B, $M_w = 7.6$). Several investigators (e.g., Protti et al. 2001, Iinuma et al. 2004, Norabuena et al. 2004, Feng et al. 2012) recognized the fairly regular occurrence of large earthquakes in this region in the past century, the latest being an $M_s = 7.7$ earthquake in 1950. These investigators initiated GPS monitoring around the Nicoya Peninsula, where these earthquakes occurred, and mapped the amount of strain accumulating on the plate boundary (**Figure 7*b***). On the basis of this map, several investigators forecasted that an $M_w = 7.5$ to 7.8 earthquake could occur in this area. Then, on September 5, 2012, an $M_w = 7.6$ earthquake occurred very close to the area where the largest strain accumulation had been mapped. At 7.8, the magnitude of the event was slightly smaller than expected, but the forecast was within a reasonable range.

Unlike these cases, the case of the 2011 Tohoku-Oki earthquake is generally considered a failure. However, it is important to investigate why this case was challenging. For the subduction zone off the Tohoku Coast, many GPS studies had previously been conducted in which onshore GPS data were extensively modeled (e.g., Ito et al. 2000, Mazzotti et al. 2000, Nishimura et al. 2004, Suwa et al. 2006, Hashimoto et al. 2009, Loveless & Meade 2010). All results indicated evidence for large strain accumulation offshore (**Figure 7*c***). However, because of the limited spatial coverage (i.e., only onshore) of strain measurements, the location of strain accumulation could not be determined very well, especially in the east–west direction. Furthermore, because of the absence, or irregular occurrence, of large historical earthquakes, the boundary conditions were not well understood. Another difficulty was that the mechanical or frictional properties of the plate boundary in Tohoku appeared to be more heterogeneous and complex than those in Chile or Costa Rica. In Chile, the plate coupling is uniformly strong, and the assumption of a stuck plate

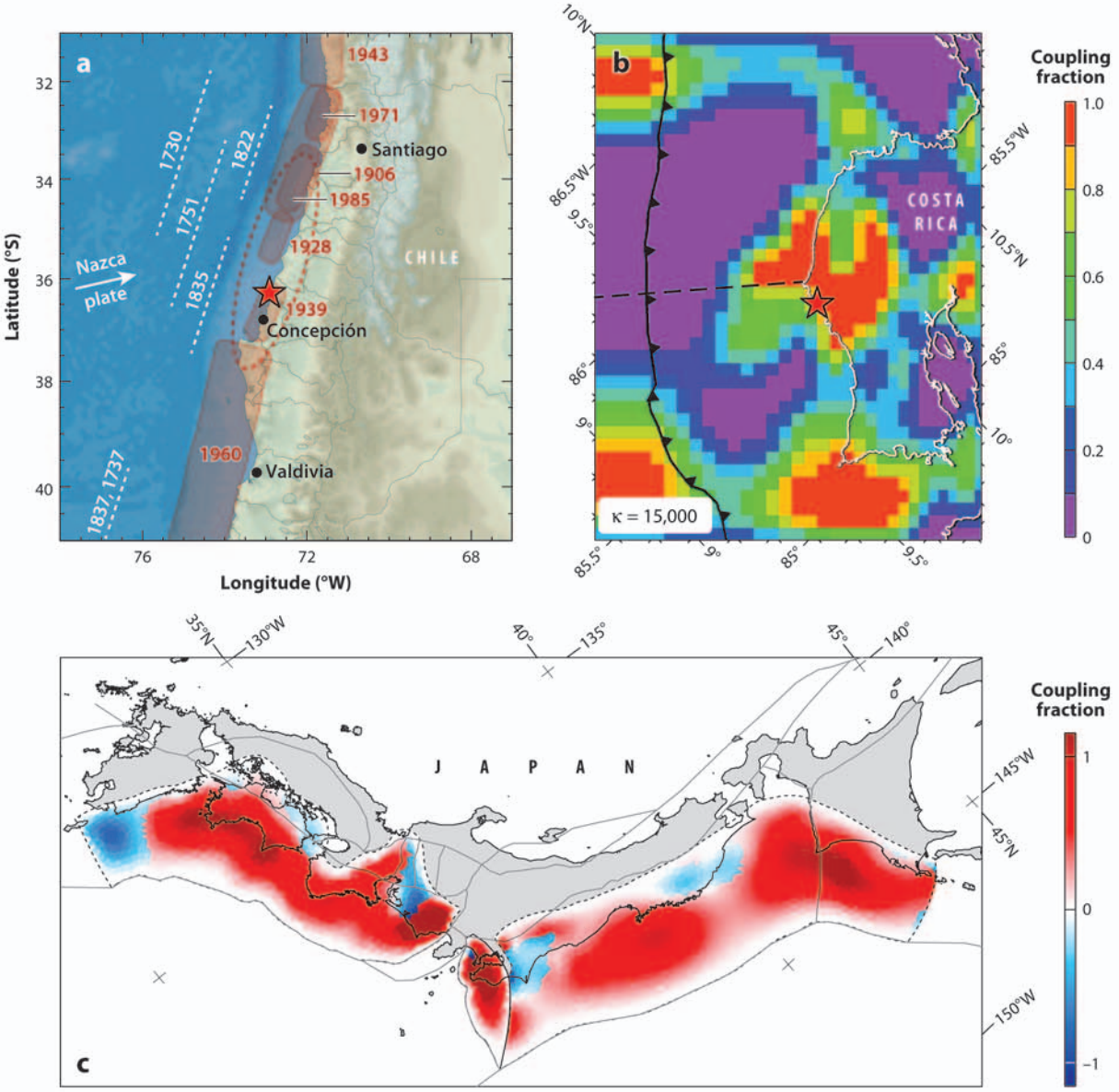

Figure 7

(*a*) The 2010 Maule, Chile, earthquake (*red star*) and rupture zones of historical Chilean earthquakes. The red dashed oval indicates the aftershock area. Although this region extends north to the 1985 rupture area, the aftershocks there may have been in the upper plate, and it may not represent the slip area on the plate boundary. The 1939 earthquake was an intraslab earthquake and probably did not rupture on the megathrust boundary (Beck et al. 1998; base map from Lay 2011). The white arrow indicates the direction of motion of the Nazca plate with respect to the South American plate. (*b*) The plate coupling map for Costa Rica (Feng et al. 2012) and the epicenter of the September 5, 2012, Costa Rica earthquake (*red star*). (*c*) Map of plate coupling off the shore of the Tohoku Coast estimated from GPS data (Loveless & Meade 2010). Thin gray lines indicate the block geometry used by Loveless & Meade (2010).

boundary seemed generally valid. In Tohoku, however, the plate coupling is spatially patchy, and the slip behavior seems to depend on the timescale of loading, as suggested by the schematic diagram in figure 2 of Lay & Kanamori (2011). The details of this phenomenon are still debated, and more research is clearly needed. In Tohoku, the strain accumulation before the Tohoku-Oki earthquake was much farther offshore than seismologists had thought. Simultaneous failure of multiple asperities also made the earthquake much larger than expected. Thus, the general approach (i.e., to understand the plate boundary structure and to measure strain accumulation) was right, but the lack of knowledge about the strength distribution and the frictional constitutive relation on the plate boundary interface resulted in a gross underestimate of the future earthquake's potential magnitude. It should also be noted that the 2011 Tohoku-Oki earthquake involved domain A, for which, as discussed above, the strain accumulation and release process is poorly known. Thus, forecasting is more difficult than it is for domain B earthquakes, which have much shorter repeat times. This example amply demonstrates the difficulty in forecasting with limited knowledge. Nevertheless, as we improve our knowledge by taking ocean-bottom measurements and by studying many earthquakes in other tectonic environments, we will be able to reduce these uncertainties.

As discussed above, scientific forecasts of domain B earthquakes are becoming feasible, at least in some subduction zones, but because of the numerous elements involved in the fracture process, any forecast is bound to be uncertain. Thus, the earthquake forecasting described here is different from the earthquake prediction perceived by the general public. Scientific forecasts of earthquakes are nevertheless important for formulating effective long-term engineering practices to mitigate seismic and tsunami hazards. Unfortunately, no matter how well we understand the basic physics of earthquakes, because of the stochastic nature of the earthquake process, unexpected rare events are inevitable and will continue to surprise seismologists. This is even truer for domain A, I, and II earthquakes, for which the underlying strain accumulation process is still uncertain and much longer timescales are involved. Given the inevitable uncertainties, it is essential to prepare for such unexpected events using the best available scientific knowledge and technology. I discuss some promising directions in the following sections.

HAZARD MITIGATION MEASURES

Earthquakes in different domains have very different source characteristics, and their occurrences have widely different timescales; thus, they have significantly different hazard implications that require different mitigation measures.

Ground-Motion Hazard

Ground-motion hazard is commonly discussed in the engineering literature; here, I focus on a few cases that are especially relevant to the diversity of earthquakes.

Since the 1960s, the number of high-rise buildings has increased dramatically. During the 1960s, seismologists commonly held two beliefs: (*a*) the magnitude of earthquakes has an upper bound at approximately 8.6, and (*b*) seismic ground motions do not contain large long-period (longer than a few seconds) components. Thus, tall buildings with a long natural period (as a rule of thumb, the natural period in seconds is approximately equal to 0.1 times the number of stories) exceeding a few seconds were considered less susceptible to common seismic ground motions with period shorter than 1 s. Since then, many seismological observations have demonstrated that the magnitude of some earthquakes exceeds 8.6. At least eight earthquakes with $M_w \geq 8.6$ have

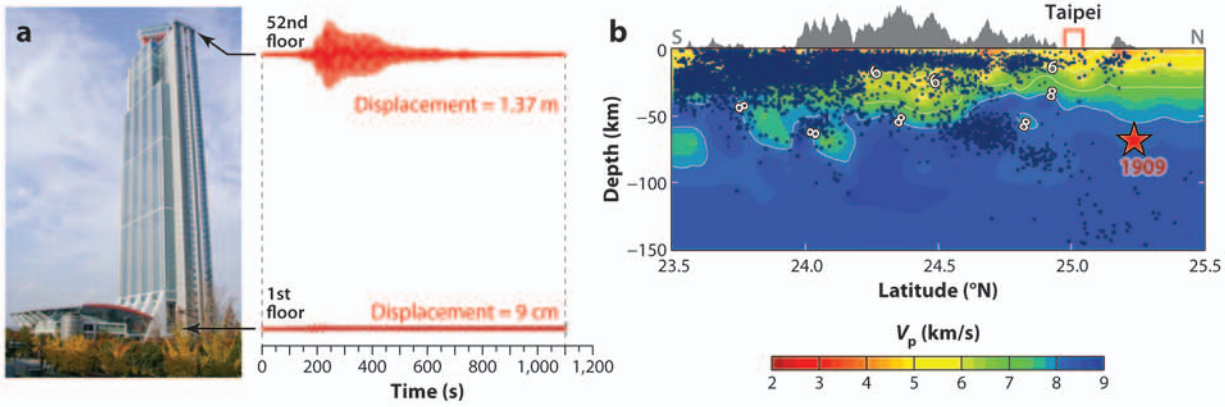

Figure 8

(*a*) Shaking of a 52-story building in Osaka Bay during the 2011 Tohoku-Oki earthquake. Displacements in the direction of the shorter dimension of the building are shown. (*b*) The 1909 intraslab earthquake in the Philippine Sea plate subducting beneath Taipei (Kanamori et al. 2012).

occurred during the past six decades. Furthermore, large long-period ground motions have been recorded for some earthquakes. For example, at a station close to the Chelungpu fault, which ruptured during the 1999 Chi-Chi, Taiwan, earthquake, the ground-motion velocity exceeded 2.5 m/s at a period of approximately 3 s (e.g., Huang et al. 2000).

Because meticulous engineering precautions are taken in the design and construction of high-rise buildings, their seismic safety should not be questioned without careful evaluations. However, there seem to be some seismological issues that warrant investigation. One example is the case of the Sakishima Building in Osaka during the 2011 Tohoku-Oki earthquake. This is a 52-story building with a height of 252 m, built in the Osaka Bay in 1997. During the Tohoku-Oki earthquake, the roof of this building swayed 1.37 m one way, even though it was as far as 800 km from the epicenter (see **Figure 8*a***) (e.g., Kashima et al. 2012). Although it did not cause serious structural damage, such large-amplitude shaking was not anticipated by building experts. Strong-motion records clearly indicate a large amplification of a factor, of approximately 30, in the Osaka basin, and because the period of the building, 6 s, matched the dominant period of the Osaka basin, the ground motion was further amplified by a factor of approximately 14 from the bottom of the building to the roof. Although this interpretation is qualitatively correct, why such a large amplification occurred has not yet been quantitatively explained. It is important to realize that large earthquakes closer to Osaka may cause even larger ground motions there than the Tohoku-Oki earthquake did. Also, the diversity of the source spectrum (**Figure 2*c***) suggests that large outer rise earthquakes and intraplate earthquakes may cause stronger ground motions than the Tohoku-Oki earthquake did, even if their magnitude is smaller. Thus, it would be prudent to explicitly consider the diversity of the source spectrum for the design and siting of high-rise buildings and other critical structures.

Another important issue is the shaking hazard caused by intraslab earthquakes. As shown in **Figure 2*c***, intraslab earthquakes have strong high-frequency radiation. Because these earthquakes are relatively infrequent and of moderate magnitude, they are not given serious consideration in hazard mitigation programs. However, as illustrated by the 1939 Chillán, Chile, earthquake and the 2011 Miyagi-Oki earthquake (**Figure 6**), intraslab earthquakes pose a significant shaking hazard if they occur underneath large cities. For example, an $M \approx 7$ earthquake occurred in 1909 in the subducted Philippine Sea plate directly beneath Taipei at a depth of approximately 70 km

(**Figure 8*b***). This type of earthquake, especially if the magnitude is larger, can be very hazardous to old structures, and it would be prudent to take the necessary precautionary actions.

Scenario Earthquake Approach

As demonstrated above, large earthquakes can now be forecasted on the basis of past seismicity, GPS measurements, and detailed studies on the earthquake rupture process. Then, scenario earthquake models can be constructed based on these forecasts. The forecasts are still subject to large uncertainties, and a single definitive scenario earthquake model is not possible; it is important to consider a range of models, rather than just a single model, for the target event. Examples of scenario earthquake models include those for great earthquakes along the Nankai trough in southwest Japan. A problem with this practice is the difficulty of setting the upper bounds of the models, because there is always a finite probability of rare outliers. Thus, when the information is released to the public, such outliers must be explicitly mentioned.

Tsunami Warning

Tsunami warning involves several components: (*a*) rapid seismic identification of the location, depth, size, and mechanism of the event; (*b*) verification and modeling of tsunamis (water waves) using deep-ocean pressure gauges and GPS wave gauges; (*c*) establishment of infrastructures for sending and receiving tsunami warnings and for executing emergency operations; and (*d*) education and training of the public. All of these elements are equally important, but in the context of this article I focus only on rapid seismic identification. For more details, many references are available—for example, a report from the US National Research Council (2011).

During the 2011 Tohoku-Oki earthquake, the Japan Meteorological Agency (JMA) issued tsunami warnings on the basis of their estimate of seismic magnitude, $M = 7.9$, roughly three minutes after the origin time of the earthquake. They warned of tsunamis with 6 m amplitude along the coast of the Miyagi prefecture and with 3 m amplitude along the coasts of the Iwate and Fukushima prefectures. This rapid warning was quite an accomplishment and probably saved many lives (Heki 2011). Although it is difficult to estimate exactly how many lives were saved, this type of warning is critically important. However, some reports have indicated that because the JMA underestimated the magnitude and, consequently, the tsunami height, many residents believed that the 6 m tsunami walls in the area would protect them from the tsunamis, did not act quickly enough, and lost their lives. If JMA could have rapidly determined the correct magnitude, $M_w = 9$, and the correct mechanism, they would have been able to issue a warning for tsunamis larger than 10 m along the entire Tohoku Coast, thereby saving substantially more lives.

With the advent of broadband seismic networks, both global and regional, it is now feasible for seismologists to rapidly determine the magnitude and the mechanism of earthquakes. It is especially important to determine the magnitude at very long period to avoid underestimation of the magnitude of tsunami earthquakes, which are deficient in high-frequency energy. The National Earthquake Information Center (NEIC) of the US Geological Survey routinely determines these parameters for earthquakes around the world. During the Tohoku-Oki earthquake, the NEIC was able to determine a preliminary magnitude of $M_w = 9.0$ and the correct thrust mechanism within approximately 20 min of the origin time (Hayes et al. 2011) using very long-period waves. If this information had been used for tsunami emergency services in Japan, it would have had a major impact on saving lives. Ideally, the JMA wants to be able to issue warning within a few minutes to enable effective emergency services. For the 2011 Tohoku-Oki earthquake, devastating tsunamis

arrived on the coast of the Iwate and Miyagi prefectures after 30 min and 1 h, respectively. Thus, if reliable seismic identification were made within a few minutes, it would have provided sufficient time for verification and effective emergency services. Determining these seismic parameters in a few minutes would be within the reach of present technology if existing regional seismic data were made available online for this purpose. Because seismic waves arrive at these stations within 3 min after the origin time, seismologists would be able to determine the necessary source parameters within a few minutes. Thus, very effective seismic tsunami warning methods are now technically available and are just waiting for implementation.

More recent studies demonstrate that the use of GPS data and local tsunami and pressure gauges would enable seismologists to estimate the spatial extent of the source region, thereby allowing more accurate and robust warnings in the very near future (Tsushima et al. 2011, Crowell et al. 2012, Ohta et al. 2012, Singh et al. 2012).

Earthquake Early Warning System

Earthquake early warning (EEW) is far more difficult than tsunami warning because a much faster response is required for the warning to be effective. Because EEW and its recent developments have been summarized in several recent publications (e.g., Kanamori 2005, Gasparini et al. 2007, Allen et al. 2009), here I discuss only its future directions. Several working and prototype systems have already been developed and employed by various users—including members of the public, through their cell phones. However, in most cases, only sites at some distance away from the source can receive the warnings; sites near the epicenter cannot receive them in time. These sites experience the most severe shaking and need warnings most desperately. In addition, with the exception of a few cases, the information is not automatically linked to the systems that need to be protected. To promote the effective use of EEW, the development of a rapid warning system that can be automatically linked to engineered systems should be encouraged. In fact, the Japanese bullet train successfully uses warnings from its own system. During the 2011 Tohoku-Oki earthquake, 24 trains were running in the Tohoku Shinkansen system. When 9 seismic sensors along the coast and 44 sensors along the train track detected the initial P wave, the power automatically shut down and the emergency brakes activated to stop all the trains, thereby avoiding derailment.

To shorten the response time, it is essential to automatically link an EEW to a structure equipped with a self-control mechanism. Some private companies have already developed such a setup. For example, one such system, upon receiving onsite warnings, protects a laser apparatus used to transcribe electronic circuits onto a computer board. Excessively strong shaking could severely damage this delicate machinery, which could result in long periods of downtime for repair.

The key challenge in designing EEW systems is how to increase reliability. The system must be sufficiently intelligent to identify the P wave and discriminate it from noise (both natural and man-made). Close collaboration among seismologists, engineers, and computer scientists is critically important for such development.

CONCLUSION

Thanks to the advent of broadband seismology and GPS, significant diversity in the source radiation spectra of large earthquakes in different subduction-zone domains has been clearly demonstrated. This diversity is the key not only to understanding the earthquake behavior of various subduction zones but also to formulating effective long-term hazard mitigation

programs. Furthermore, seismologists' ability to forecast future large earthquakes depends on the complexity of the plate boundary structures. The successful forecasts of the 2010 Maule, Chile, earthquake and the 2012 Costa Rica earthquake are encouraging, but the inevitable uncertainties, which arise from the complexity of the rupture process, must be kept in mind. Advancements in real-time seismology give seismologists hope that they can effectively deal with these uncertainties. Maximizing the utility of a real-time system for damage mitigation will require cross-disciplinary efforts among science, engineering, and government organizations.

DISCLOSURE STATEMENT

The author is not aware of any affiliations, memberships, funding, or financial holdings that might be perceived as affecting the objectivity of this review.

ACKNOWLEDGMENTS

I thank Luis Rivera and Toru Matsuzawa, who kindly read the final manuscript and provided me with many useful suggestions for improvement. The IRIS DMS data center was used to access the seismic data from Global Seismic Network and Federation of Digital Seismic Network Stations. The F-net, K-NET, and KiK-net data were obtained from the National Research Institute for Earth Science and Disaster Prevention (NIED) data centers.

LITERATURE CITED

Abercrombie RE, Antolik M, Felzer K, Ekström G. 2001. The 1994 Java tsunami earthquake: slip over a subducting seamount. *J. Geophys. Res.* 106:6595–607

Aki K. 1967. Scaling law of seismic spectrum. *J. Geophys. Res.* 72:1217–31

Allen RM, Gasparini P, Kamigaichi O, Böse M. 2009. The status of earthquake early warning around the world: an introductory overview. *Seismol. Res. Lett.* 80:682–93

Ammon CJ, Kanamori H, Lay T. 2008. A great earthquake doublet and seismic stress transfer cycle in the central Kuril islands. *Nature* 451:561–65

Ammon CJ, Kanamori H, Lay T, Velasco AA. 2006. The 17 July 2006 Java tsunami earthquake. *Geophys. Res. Lett.* 33:L24308

Ando M. 1975. Source mechanisms and tectonic significance of historical earthquakes along the Nankai trough, Japan. *Tectonophysics* 27:119–40

Asano K, Iwata T, Irikura K. 2004. Source modeling and strong ground motion simulation of the off Miyagi intraslab earthquake of May 26, 2003. *Zisin* 57:171–85 (In Japanese)

Bak P, Tang C. 1989. Earthquakes as self-organized critical phenomena. *J. Geophys. Res.* 94:15635–37

Beavan J, Wang X, Holden C, Wilson K, Power W, et al. 2010. Near-simultaneous great earthquakes at Tongan megathrust and outer rise in September 2009. *Nature* 466:959–63

Beck S, Barrientos S, Kausel E, Reyes M. 1998. Source characteristics of historic earthquakes along the central Chile subduction zone. *J. S. Am. Earth Sci.* 11:115–29

Brune JN. 1970. Tectonic stress and the spectra of seismic shear waves from earthquakes. *J. Geophys. Res.* 75:4997–5009

Christensen DH, Ruff L. 1988. Seismic coupling and outer rise earthquakes. *J. Geophys. Res.* 93:13421–44

Cisternas M, Atwater BF, Torrejon F, Sawai Y, Machuca G, et al. 2005. Predecessors of the giant 1960 Chile earthquake. *Nature* 437:404–7

Crowell BW, Bock Y, Melgar D. 2012. Real-time inversion of GPS data for finite fault modeling and rapid hazard assessment. *Geophys. Res. Lett.* 39:L09305

Darwin C. 1845. *Journal of Researches into the Natural History and Geology of the Countries Visited during the Voyage of H.M.S. Beagle Round the World.* London: John Murray

Delouis B, Nocquet J-M, Vallée M. 2010. Slip distribution of the February 27, 2010 $M_w = 8.8$ Maule earthquake, central Chile, from static and high-rate GPS, InSAR, and broadband teleseismic data. *Geophys. Res. Lett.* 37:L17305

Fedotov SA. 1965. Regularities of the distribution of strong earthquakes in Kamchatka, the Kuril islands and northeastern Japan. *Tr. Inst. Fiz. Zemli Akad. Nauk SSSR* 36:66–93 (In Russian)

Feng L, Newman AV, Protti M, González V, Jiang Y, Dixon TH. 2012. Active deformation near the Nicoya Peninsula, northwestern Costa Rica, between 1996 and 2010: interseismic megathrust coupling. *J. Geophys. Res.* 117:B06407

Gasparini P, Manfredi G, Zschau J. 2007. *Earthquake Early Warning Systems*. Berlin: Springer

Hackl M, Malservisi R, Wdowinski S. 2009. Strain rate patterns from dense GPS networks. *Nat. Hazards Earth Syst. Sci.* 9:1177–87

Hashimoto C, Noda A, Sagiya T, Matsu'ura M. 2009. Interplate seismogenic zones along the Kuril-Japan trench inferred from GPS data inversion. *Nat. Geosci.* 2:141–44

Hayes GP, Earle PS, Benz HM, Wald DJ, Briggs RW, USGS/NEIC Earthq. Response Team. 2011. 88 hours: the US Geological Survey National Earthquake Information Center response to the 11 March 2011 M_w 9.0 Tohoku earthquake. *Seismol. Res. Lett.* 82:481–93

Heki K. 2011. A tale of two earthquakes. *Science* 332:1390–91

Hill EM, Borrero JC, Huang Z, Qiu Q, Banerjee P, et al. 2012. The 2010 M_w 7.8 Mentawai earthquake: very shallow source of a rare tsunami earthquake determined from tsunami field survey and near-field GPS data. *J. Geophys. Res.* 117:B06402

Hsu Y-J, Simons M, Avouac J-P, Galetzka J, Sieh K, et al. 2006. Frictional afterslip following the 2005 Nias-Simeulue earthquake, Sumatra. *Science* 312:1921–26

Huang B-S, Chen K-C, Huang W-G, Wang J-H, Chang T-M, et al. 2000. Characteristics of strong ground motion across a thrust fault tip from the September 21, 1999, Chi-Chi, Taiwan earthquake. *Geophys. Res. Lett.* 27:2729–32

Ide S, Takeo M. 1996. The dynamic rupture process of the 1993 Kushiro-Oki earthquake. *J. Geophys. Res.* 101(B3):5661–75

Iinuma T, Protti M, Obana K, González V, Van der Laat R, et al. 2004. Inter-plate coupling in the Nicoya Peninsula, Costa Rica, as deduced from a trans-peninsula GPS experiment. *Earth Planet. Sci. Lett.* 223:203–12

Imamura A. 1928. On the seismic activity of central Japan. *Jap. J. Astron. Geophys.* 6:119–37

Ito T, Yoshioka S, Miyazaki Si. 2000. Interplate coupling in northeast Japan deduced from inversion analysis of GPS data. *Earth Planet. Sci. Lett.* 176:117–30

Kagan YY, Jackson DD. 1991. Seismic gap hypothesis: ten years after. *J. Geophys. Res.* 96(B13):21419–31

Kanamori H. 1970. The Alaska earthquake of 1964: radiation of long-period surface waves and source mechanism. *J. Geophys. Res.* 75:5029–40

Kanamori H. 1971. Seismological evidence for a lithospheric normal faulting—the Sanriku earthquake of 1933. *Phys. Earth Planet. Inter.* 4:289–300

Kanamori H. 1972. Mechanism of tsunami earthquakes. *Phys. Earth Planet. Inter.* 6:346–59

Kanamori H. 2005. Real-time seismology and earthquake damage mitigation. *Annu. Rev. Earth Planet. Sci.* 33:195–214

Kanamori H, Anderson DL. 1975. Theoretical basis of some empirical relations in seismology. *Bull. Seismol. Soc. Am.* 65:1073–95

Kanamori H, Kikuchi M. 1993. The 1992 Nicaragua earthquake: a slow tsunami earthquake associated with subducted sediments. *Nature* 361:714–16

Kanamori H, Lee WHK, Ma K-F. 2012. The 1909 Taipei earthquake—implication for seismic hazard in Taipei. *Geophys. J. Int.* 191:126–46

Kanamori H, Rivera L, Lee WHK. 2010. Historical seismograms for unravelling a mysterious earthquake: the 1907 Sumatra earthquake. *Geophys. J. Int.* 183:358–74

Kashima T, Koyama S, Okawa I. 2012. *Strong motion records in buildings from the 2011 off the Pacific coast of Tohoku earthquake*. Build. Res. Data No. 135, Build. Res. Inst., Tsukuba, Japan

Kelleher J, Savino J, Rowlett H, McCann W. 1974. Why and where great thrust earthquakes occur along island arcs. *J. Geophys. Res.* 79:4889–99

Konca AO, Avouac J-P, Sladen A, Meltzner AJ, Sieh K, et al. 2008. Partial rupture of a locked patch of the Sumatra megathrust during the 2007 earthquake sequence. *Nature* 456:631–35

Lay T. 2011. Earthquakes: a Chilean surprise. *Nature* 471:174–75

Lay T, Ammon CJ, Kanamori H, Koper KD, Sufri O, Hutko AR. 2010a. Teleseismic inversion for rupture process of the 27 February 2010 Chile (M_w 8.8) earthquake. *Geophys. Res. Lett.* 37:L13301

Lay T, Ammon CJ, Kanamori H, Rivera L, Koper KD, Hutko AR. 2010b. The 2009 Samoa-Tonga great earthquake triggered doublet. *Nature* 466:964–68

Lay T, Ammon CJ, Kanamori H, Yamazaki Y, Cheung KF, Hutko AR. 2011. The 25 October 2010 Mentawai tsunami earthquake (M_w 7.8) and the tsunami hazard presented by shallow megathrust ruptures. *Geophys. Res. Lett.* 38:L06302

Lay T, Kanamori H. 1980. Earthquake doublets in the Solomon Islands. *Phys. Earth Planet. Inter.* 21:283–304

Lay T, Kanamori H. 1981. An asperity model of large earthquake sequences. In *Earthquake Prediction: An International Review*, ed. DW Simpson, PG Richards, pp. 579–92. Washington, DC: AGU

Lay T, Kanamori H. 2011. Insights from the great 2011 Japan earthquake. *Phys. Today* 64:33–39

Lay T, Kanamori H, Ammon CJ, Koper KD, Hutko AR, et al. 2012. Depth-varying rupture properties of subduction zone megathrust faults. *J. Geophys. Res.* 117:B04311

Lomnitz C. 2004. Major earthquakes of Chile: a historical survey, 1535–1960. *Seismol. Res. Lett.* 75:368–78

Lorito S, Romano F, Atzori S, Tong X, Avallone A, et al. 2011. Limited overlap between the seismic gap and coseismic slip of the great 2010 Chile earthquake. *Nat. Geosci.* 4:173–77

Loveless JP, Meade BJ. 2010. Geodetic imaging of plate motions, slip rates, and partitioning of deformation in Japan. *J. Geophys. Res.* 115:B02410

Lynnes CS, Lay T. 1988. Source process of the great 1977 Sumba earthquake. *J. Geophys. Res.* 93:13407–20

Mazzotti S, Le Pichon X, Henry P, Miyazaki S-I. 2000. Full interseismic locking of the Nankai and Japan–west Kurile subduction zones: an analysis of uniform elastic strain accumulation in Japan constrained by permanent GPS. *J. Geophys. Res.* 105(B6):13159–77

McCann WR, Nishenko SP, Sykes LR, Krause J. 1979. Seismic gaps and plate tectonics; seismic potential for major boundaries. *Pure Appl. Geophys.* 117:1082–147

Mogi K. 1968. Some features of recent seismic activity in and near Japan, 1. *Bull. Earthq. Res. Inst. Tokyo Univ.* 46:1225–36

Morikawa N, Sasatani T. 2003. Source spectral characteristics of two large intra-slab earthquakes along the southern Kuril-Hokkaido arc. *Phys. Earth Planet. Inter.* 137:67–80

Nakajima J, Hasegawa A, Kita S. 2011. Seismic evidence for reactivation of a buried hydrated fault in the Pacific slab by the 2011 M9.0 Tohoku earthquake. *Geophys. Res. Lett.* 38:L00G6

National Research Council. 2011. *Tsunami Warning and Preparedness: An Assessment of the US Tsunami Program and the Nation's Preparedness Efforts*. Washington, DC: Natl. Acad. Press

Newcomb KR, McCann WR. 1987. Seismic history and seismotectonics of the Sunda arc. *J. Geophys. Res.* 92:421–39

Newman AV, Hayes G, Wei Y, Convers JA. 2011. The 25 October 2010 Mentawai tsunami earthquake, from real-time discriminants, finite fault rupture, and tsunami excitation. *Geophys. Res. Lett.* 38:L05302

Newman AV, Okal EA. 1998. Teleseismic estimates of radiated seismic energy: the E/M_0 discriminant for tsunami earthquakes. *J. Geophys. Res.* 103:26885–98

Nishenko SP, Sykes LR. 1993. Comment on "Seismic gap hypothesis: ten years after" by Y.Y. Kagan and D.D. Jackson. *J. Geophys. Res.* 98(B6):9909–16

Nishimura T, Hirasawa T, Miyazaki Si, Sagiya T, Tada T, et al. 2004. Temporal change of interplate coupling in northeastern Japan during 1995–2002 estimated from continuous GPS observations. *Geophys. J. Int.* 157:901–16

Norabuena E, Dixon TH, Schwartz S, DeShon H, Newman A, et al. 2004. Geodetic and seismic constraints on some seismogenic zone processes in Costa Rica. *J. Geophys. Res.* 109:B11403

Ohta Y, Kobayashi T, Tsushima H, Miura S, Hino R, et al. 2012. Quasi real-time fault model estimation for near-field tsunami forecasting based on RTK-GPS analysis: application to the 2011 Tohoku-Oki earthquake (M_w 9.0). *J. Geophys. Res.* 117:B02311

Ohta Y, Miura S, Ohzono M, Kita S, Iinuma T, et al. 2011. Large intraslab earthquake (2011 April 7, *M* 7.1) after the 2011 off the Pacific coast of Tohoku earthquake (*M* 9.0): coseismic fault model based on the dense GPS network data. *Earth Planets Space* 63:1207–11

Otsuka M. 1972. A chain-reaction type source model as a tool to interpret the magnitude frequency relation of earthquakes. *J. Phys. Earth* 20:35–45

Philibosian B, Sieh K, Natawidjaja DH, Chiang H-W, Shen C-C, et al. 2012. An ancient shallow slip event on the Mentawai segment of the Sunda megathrust, Sumatra. *J. Geophys. Res.* 117:B05401

Plafker G, Rubin M. 1978. *Uplift history and earthquake recurrence as deduced from marine terraces on Middleton Island, Alaska.* USGS Open-File Rep. 78-943, USGS, Reston, VA

Polet J, Kanamori H. 2000. Shallow subduction zone earthquakes and their tsunamigenic potential. *Geophys. J. Int.* 142:684–702

Polet J, Kanamori H. 2009. Tsunami earthquakes. In *Encyclopedia of Complexity and Systems Science*, ed. RA Meyers. New York: Springer

Polet J, Thio HK. 2003. The 1994 Java tsunami earthquake and its "normal" aftershocks. *Geophys. Res. Lett.* 30:1474

Press F. 1961. Experimental determination of earthquake fault length and rupture velocity. *J. Geophys. Res.* 66:3471–85

Protti M, Guendel F, Malavassi E. 2001. *Evaluacion del Potencial Sismico de la Peninsula de Nicoya*. Heredia, Costa Rica: Ed. Fund. UNA. 1st ed.

Ruegg JC, Campos J, Madariaga R, Kausel E, de Chabalier JB, et al. 2002. Interseismic strain accumulation in south central Chile from GPS measurements, 1996–1999. *Geophys. Res. Lett.* 29:12–1–4

Ruegg JC, Rudloff A, Vigny C, Madariaga R, de Chabalier JB, et al. 2009. Interseismic strain accumulation measured by GPS in the seismic gap between Constitución and Concepción in Chile. *Phys. Earth Planet. Inter.* 175:78–85

Sagiya T. 2004. A decade of GEONET: 1994–2003. The continuous GPS observation in Japan and its impact on earthquake studies. *Earth Planets Space* 56:xxix–xli

Saint-Amand P. 1961. *Los terremotos de Mayo, Chile 1960*. Tech. Article 14, Michelson Lab., US Nav. Ordnance Test Stn., China Lake, CA

Sieh K, Natawidjaja DH, Meltzner AJ, Shen C-C, Cheng H, et al. 2008. Earthquake supercycles inferred from sea-level changes recorded in the corals of west Sumatra. *Science* 322:1674–78

Singh SK, Pérez-Campos X, Iglesias A, Melgar D. 2012. A method for rapid estimation of moment magnitude for early tsunami warning based on coastal GPS networks. *Seismol. Res. Lett.* 83:516–30

Spence W. 1986. The 1977 Sumba earthquake series: evidence for slab pull force acting at a subduction zone. *J. Geophys. Res.* 91(B7):7225–39

Stauder W. 1968a. Mechanism of the Rat Island earthquake sequence of 4 February 1965 with relation to island arcs and sea-floor spreading. *J. Geophys. Res.* 73:3847–58

Stauder W. 1968b. Tensional character of earthquake foci beneath the Aleutian trench with relation to sea-floor spreading. *J. Geophys. Res.* 73:7693–701

Suwa Y, Miura S, Hasegawa A, Sato T, Tachibana K. 2006. Interplate coupling beneath NE Japan inferred from three-dimensional displacement field. *J. Geophys. Res.* 111:B04402

Suzuki W, Aoi S, Sekiguchi H. 2009. Rupture process of the 2008 Northern Iwate intraslab earthquake derived from strong-motion records. *Bull. Seismol. Soc. Am.* 99:2825–35

Sykes LR. 1972. Seismicity as a guide to global tectonics and earthquake prediction. *Tectonophysics* 13:393–414

Tsuboi C. 1932. Investigation on the deformation of the Earth's crust in the Tango district connected with the Tango earthquake of 1927 (Part 4). *Bull. Earthq. Res. Inst. Tokyo Univ.* 10:411–34

Tsushima H, Hirata K, Hayashi Y, Tanioka Y, Kimura K, et al. 2011. Near-field tsunami forecasting using offshore tsunami data from the 2011 off the Pacific coast of Tohoku earthquake. *Earth Planets Space* 63:821–26

Uchida N, Matsuzawa T, Ellsworth WL, Imanishi K, Okada T, Hasegawa A. 2007. Source parameters of a M4.8 and its accompanying repeating earthquakes off Kamaishi, NE Japan: implications for the hierarchical structure of asperities and earthquake cycle. *Geophys. Res. Lett.* 34:L20313

Vere-Jones D. 1976. A branching model for crack propagation. *Pure Appl. Geophys.* 114:711–25

Vigny C, Socquet A, Peyrat S, Ruegg J-C, Métois M, et al. 2011. The 2010 M_w 8.8 Maule megathrust earthquake of central Chile, monitored by GPS. *Science* 332:1417–21

Ye L, Lay T, Kanamori H. 2012. Intraplate and interplate faulting interactions during the August 31, 2012, Philippine Trench earthquake (M_w 7.6) sequence. *Geophys. Res. Lett.* 39:L24310

Ye L, Lay T, Kanamori H. 2013. Ground shaking and seismic source spectra for large earthquakes around the megathrust fault offshore of northeastern Honshu, Japan. *Bull. Seismol. Soc. Am.* 103:1221–41

Yomogida K, Yoshizawa K, Koyama J, Tsuzuki M. 2011. Along-dip segmentation of the 2011 off the Pacific coast of Tohoku earthquake and comparison with other megathrust earthquakes. *Earth Planets Space* 63:697–701